Signals for a Transition from Surface to Bulk Emission in Thermal Multifragmentation

L. Beaulieu,[1] T. Lefort,[1] K. Kwiatkowski,[1*] R.T. de Souza,[1] W.-c. Hsi,[1] L. Pienkowski,[2] B. Back,[3] D.S. Bracken,[1,+] H. Breuer,[4] E. Cornell,[1 ‡] F. Gimeno-Nogues,[5] D.S. Ginger,[1§] S. Gushue,[6] R.G. Korteling,[7] R. Laforest,[5**] E. Martin,[5] K.B. Morley,[2] E. Ramakrishnan,[5] L.P. Remsberg,[6] D. Rowland,[5] A. Ruangma,[5] V.E. Viola,[1] G. Wang,[1†] E. Winchester[5] and S.J. Yennello[5]

[1]*Department of Chemistry and IUCF, Indiana University, Bloomington, IN 47405*
[2]*Heavy Ion Laboratory, Warsaw University, Warsaw Poland*
[3]*Physics Division, Argonne National Laboratory, Argonne IL 60439*
[4]*Department of Physics, University of Maryland, College Park, MD 20740*
[5]*Department of Chemistry & Cyclotron Laboratory, Texas A&M University, College Station, TX 77843*
[6]*Chemistry Department, Brookhaven National Laboratory, Upton, NY 11973*
[7]*Department of Chemistry, Simon Fraser University, Burnaby, BC. Canada V5A IS6*

(September 15, 2018)

Abstract

Excitation-energy-gated two-fragment correlation functions have been studied between 2 to 9A MeV of excitation energy for equilibrium-like sources formed in π^- and p + ^{197}Au reactions at beam momenta of 8,9.2 and 10.2 GeV/c. Comparison of the data to an N-body Coulomb-trajectory code shows a decrease of one order of magnitude in the fragment emission time in the excitation energy interval 2-5A MeV, followed by a nearly constant breakup time at higher excitation energy. The observed decrease in emission time is shown to be strongly correlated with the increase of the fragment emission probability, and the onset of thermally-induced radial expansion. This result is interpreted as evidence consistent with a transition from surface-dominated

*Present address: Los Alamos National Laboratory, Los Alamos, NM 87545

‡Present address: Lawrence Berkeley Laboratory, Berkeley, CA 94720

§Cambridge University, Cambridge, U.K.

**Barnes Hospital, Washington University, St. Louis, MO 63130

†Present address: Epsilon, Inc., Dallas, TX 75240

to bulk emission expected for spinodal decomposition.

25.70.Pq,21.65+f,25.40-h,25.80.Hp

The nuclear liquid-gas phase transition is often linked to the experimental observation of multiple intermediate mass fragments (IMF= $3 \leq Z \tilde{\leq} 20$), or multifragmentation [1]. This interpretation was preceded by the discovery of a power-law behavior in the mass (and charge) distributions of IMFs in high energy p+Xe reactions [2]. In recent years, better experimental technologies have made possible the detection and nearly complete characterization of multifragmentation reactions on an event-by-event basis. Two *stimulating* results have come from such exclusive experiments: the measurement of a latent heat for nuclear matter by Pochodzalla et al. [3], reminiscent of the liquid-gas phase transition in water,and the extraction of critical exponents for nuclear matter, in agreement with those of liquid-gas values, by the EOS collaboration [4]. While debate continues related to these findings [5–8], the important point remains that the current state of the data is suggestive of a liquid-gas phase transition, either first or second order. More recently, it has been argued that due to finite-size effects, both first- and second-order phase transition characteristics can be observed simultaneously [9].

An aspect of this phase transition that has been less systematically examined is the cluster-emission time scale involved in the transition of the nuclear liquid to a liquid-vapor coexistence phase. For cluster emission from the liquid phase, fragment formation occurs at the surface of the excited source via a binary splitting, much like fission. This process gives rise to long emission times of the order of 10^{-20} - 10^{-21} sec, necessary for shape deformation. In sharp contrast, when the spinodal boundary of the phase diagram is crossed, the system falls apart on a very short time scale ($\sim 10^{-22}$ - 10^{-23}sec); i.e. bulk emission.

Although the transition from long to short emission times has previously been reported for central heavy-ion collisions, no systematic analysis of source lifetime as a function of excitation energy per nucleon, E^*/A, has yet been performed for a single, well-defined equilibrated system. Previous studies have estimated the excitation energy scale by either fixing the target-projectile combination and varying the bombarding energy [10], or combining results from several different experiments, in which E^*/A was evaluated [11]. In both cases, there are problems in heavy-ion reactions associated with entrance-channel dynamics and with source selection, which lead to a single thermalized source for less than few percent of the total reaction cross-section [12–14].

In this letter we present the systematic evolution of IMF emission times over a wide range of excitation energy for well characterized, thermal-like sources formed in hadron-induced reactions, as described in [15,16]. This evolution is then correlated to the n-fold emission probability and to the onset of thermally-induced radial expansion. The convergence of the results suggests a transition from surface emission to bulk emission around 5A MeV of excitation energy, in good agreement with the theoretical prediction of Bondorf et al. [17].

Emission times were obtained using excitation-energy-gated two-IMF correlation functions constructed from events measured with the ISiS 4π detector array [18] during experiment E900 at the Brookhaven National Laboratory AGS accelerator. Beams of 8.0 GeV/c tagged $\pi^-$and 8.2, 9.2 GeV/c π^- and 10.2 GeV/c protons (untagged) were incident on a 1.8 mg/cm^2 ^{197}Au target. Fragments with charge Z$\leq$16 were identified with a set of 162 gas-ion chamber/Si/CsI triple telescopes with energy acceptance 1.0$\leq$E/A$\leq$92 MeV. Geometric acceptance was 74% of 4π. Further experimental details can be found in [15,19]. For all these reactions, the reconstructed primary source size, final residue size, charge distribution, fragment multiplicity and cross-section were found to be the same when selected as a function

of E^*/A [16,19]. By combining these data sets, we have access to 7 million events for which $\sim$7% contain two or more IMFs with $4 \leq Z_{imf} \leq 9$.

Emission time scales were derived using the intensity-interferometry technique [20–28], which employs two-fragment reduced-velocity correlation functions, defined as

$$R(v_{red}) + 1 = C \frac{N_{corr}(v_{red})}{N_{uncorr}(v_{red})}, \tag{1}$$

where v_{red} is the reduced relative velocity between the two fragments:

$$v_{red} = \frac{\mid \vec{v_1} - \vec{v_2} \mid}{\sqrt{Z_1 + Z_2}}. \tag{2}$$

Here v_i and Z_i are the laboratory velocity and charge of the fragments, respectively. The denominator permits comparison of different Z values [23]. $N_{corr}(v_{red})$ is the measured coincidence yield while $N_{uncorr}(v_{red})$ is the uncorrelated yield calculated using the event-mixing technique [23]. For each E^*/A bin, both the numerator and demominator were normalized to their integral and then the ratio was constructed. At large v_{red}, constant values of $R(v_{red}) + 1 \approx 1$ are found, largely due to the use of the full 4π range of the array, which enables high statistical samples of large-angle correlations.

The experimental excitation-energy-gated IMF-IMF correlation functions ($4 \leq Z_1, Z_2 \leq 9$) are shown in Fig. 1 for source excitation energies $E^*/A = 2.25 \pm 0.25$, 3.0 ± 0.5, 5.0 ± 1.0 and 8.0 ± 1.0 MeV. Yield suppression at low v_{red}, due to the Coulomb interaction between IMFs, increases with E^*/A. The increase of the Coulomb hole (yield suppression) is large between $E^*/A = 2.25$ MeV and 5 MeV of excitation energy, followed by a nearly constant yield suppression for higher excitation energies. This effect is in agreement with previous analyses that have selected the most central collisions of a given reaction and varied the bombarding energy [10,24]. However, as discussed in the introduction, the formation of a single source in heavy-ion collisions is limited to a fraction of the cross-section, which makes the task of separating the actual thermalized source from contamination difficult. In hadron-induced reactions, there is only one source of thermalized fragments, it has little collective compressional or rotational character, and the data cover a wide range of excitation energy.

The evaluation of the emission time scale at various excitation energies is done by comparison of the data with the N-body Coulomb trajectory code of Glasmacher *et al* [26,27]. Because the starting source size, as well as the final residue size, are known, the simulation is simplified; i.e. no "empirical" adjustments of these quantities is possible, only the volume or separation distance between the residue and the fragments. The Coulomb-trajectory simulation employed in this time-scale analysis assumes sequential emission from the surface of a spherical source; thus there are no complications due to initial-state momentum correlations [27].

Two-dimensional maps of measured source charge vs. residue charge and IMF kinetic energy in source frame vs. charge are used to define the initial conditions. The filtered output of the simulation is required to reproduce both the small- and large-angle correlation data, as well as fragment kinetic-energy spectra and charge distributions. As in [28], average Coulomb-barriers are subtracted at the input for each Z, effectively sampling the exponential (thermal) part of the spectra. The Coulomb energy is calculated and added back in the simulation according to

$$V_{Coul} = \frac{1.44 Z_{IMF}\, Z_{res}}{r_o(A_{IMF}^{1/3} + A_{res}^{1/3}) + d}, \quad (3)$$

where r_o = 1.22 fm and d is an adjustable parameter that defines the source dimensions. At low excitation, a distance of 6 fm is required to reproduce the energy spectra down to 2A MeV, corresponding to IMF-residue axial separation distances consistent with fission systematics using r_0=2 fm and d=0 fm in Eq. 3. At high excitation, values of d as low as 2 fm will reproduce the energy spectra down to 1A MeV. For the purpose of comparison of the data with the calculations, correlation functions for IMF kinetic energy between 2A MeV and 10A MeV are used. Equivalently, assuming radial separation instead of axial (high excitation scenario), the above range for d (2-6 fm) would correspond to a freeze-out volume of $4V_0$-$6V_0$ ($2.5V_0$-$4V_0$) using r_0=1.22 fm (1.44 fm) as a normal density reference. Finally, the emission time t is assigned via an exponential probability distribution, $e^{-t/\tau}$, where τ is the decay lifetime.

In Fig. 2 we show fits to the correlation functions for three bins in E^*/A for a range of d and τ that yield minimum chi-squared values. Between E^*/A = 2 - 2.5 MeV and 4.5-5.5 MeV, the emission time decreases nearly an order of magnitude from ∼500 fm/c to 30-75 fm/c. Above $E^*/A \sim 5$ MeV, the emission time becomes very short (20 to 50 fm/c) and nearly independent of excitation energy, consistent with a near-instantaneous breakup, explosion-like phenomenon. As has been pointed out previously, lifetimes less than τ ∼30 fm/c become comparable to thermodynamic fluctuations in the system, as discussed in ref. [28]. Moreover, correlation functions for a similar reaction have been shown to be reproduced by a simultaneous multifragmentation model at high excitation [28], again consistent with our extracted time scale.

As in past studies, Fig. 2 provides evidence for the space-time ambiguity of the correlation function [25]. However, the difference between the various decay lifetimes at high E^*/A is rather small and agrees within the error bars. Therefore, the observed saturation in the space-time extent of the source reflects to a large degree a saturation of the decay lifetime as well.

The lower frame of Fig. 3 presents the best-fit decay times for hadron-induced thermal multifragmentation of ^{197}Au nuclei, with two extreme solutions shown above 4A MeV. The decay lifetimes evolve systematically as a function of E^*/A, extending from the evaporative regime at low E^*/A to that for multifragmentation at high E^*/A. The shaded band shows the range of space-time values for which a consistent fit to all of the observables is achieved. The solid points represent independent measurements for heavy-ion-induced reactions for which the source E^*/A has been explicitly evaluated [11]. At high excitation energies the ISiS results are similar to the heavy-ion data. However, as E^*/A decreases, longer lifetimes are derived from the heavy-ion data. The differences can possibly be explained by a better source selection in hadron-induced reaction with minimal influence from various entrance-channel collective behavior, all of which contribute to lowering the reconstructed E^*/A [16].

The solid line in the lower frame of Fig. 3 shows the best fit to an exponential function ($e^{\alpha/\sqrt{E^*/A}}$) for the ISiS data; the dashed line describes a similar fit using the heavy-ion results at low excitations. These two lines should be seen as defining upper and lower limits of the changes in emission time with E^*/A based on all available data.

In ref. [29] the thermally-driven radial expansion, ϵ_r, has been derived for the ISiS data as a function of E^*/A, based on an analysis of the fragment kinetic energy spectra. The

center frame in Fig. 3 shows that onset of thermal expansion energy for the ISiS data, which occurs around E^*/A=3.5 MeV (4.75 MeV), assuming a freeze-out density of ρ/ρ_0=1/3 (1/2). The measurements of a distinct signal for ϵ_r is interpreted as evidence that the system has reached a reduced density [29], an essential condition for bulk emission.

In the upper panel of Fig. 3 the decay lifetime systematics are compared with the probability for a given observed IMF multiplicity, N_{IMF}, as a function of E^*/A, uncorrected for ISiS efficiency. The dotted vertical lines that run across all three frames – E^*A 4.25±0.50 MeV – represent an apparent transition region in which multiple IMF emission becomes the dominant process, the onset of thermally-induced radial expansion appears, and decay times become comparable to the thermodynamic fluctuation time ($\tau < 30$ fm/c). Furthermore for the same system under study, this region in E^*/A yields the most diverse fragment size distribution (minimum power-law exponent) [16]. We interpret the simultaneous change of the various observables in this region of E^*/A as evidence supporting a transition from a surface emission mechanism (long timescales) to bulk disintegration (short timescales) in hot nuclear matter.

In summary, IMF-IMF correlation functions for hadron-induced thermal multifragmentation events have been studied in the excitation energy regime E^*/A = 2-9 MeV. The Coulomb suppression of the correlation function at low reduced velocities shows a systematic evolution with increasing heat content. Long times (minimal suppression) are associated with low excitation energies and short times with larger values (large suppression). Between E^*/A = 2 - 5 MeV, this evolution is quite strong; above 5 MeV/A the correlation functions show little change. Decay lifetimes that decrease from $\tau \sim 500$ fm/c at E^*/A = 2 MeV to $\tau \sim$ 20-50 fm/c for $E^*/A \geq 5$ MeV are derived from fits to the correlation functions with an N-body Coulomb-trajectory simulation that also reproduces the IMF kinetic-energy spectra, charge distributions and large-angle correlations. Placing this timescale evolution with E^*/A in context with similar behavior for multiple fragment production probabilities and the onset of thermally-induced radial expansion, we conclude that the data provide evidence consistent with a transition from surface to bulk emission in hot nuclear matter near E^*/A = 5 MeV.

The authors wish to thank Thomas Glasmacher for providing his N-body Coulomb-trajectory code. This work was supported by the U.S. Department of Energy and National Science Foundation, the National Sciences and Engineering Research Council of Canada, Grant No. P03B 048 15 of the Polish State Committee for Scientific Research, Indiana University Office of Research and the University Graduate School, Simon Fraser University and the Robert A. Welch Foundation.

REFERENCES

[1] L.G. Moretto and G.J. Wozniak, Ann. Rev. Nucl. Part. Sci. **43**, 379 (1993) and refs. therein.
[2] J.E. Finn *et al.*, Phys. Rev. Lett. **49**, 1321 (1982).
[3] J. Pochodzalla *et al.*, Phys. Rev. Lett. **75**, 1040 (1995).
[4] M.L. Gilkes *et al.*, Phys. Rev. Lett. **73**, 1590 (1994).
[5] B. Hauger *et al.*, Phys. Rev. Lett.**77**, 235 (1996).
[6] K. Kwiatkowski *et al.*, Phys. Lett. B **423**, 21 (1998).
[7] Y.G. Ma *et al.*, Phys. Lett. B **390**, 41 (1997).
[8] R. Wada *et al.*, Phys. Rev. C **55**, 227 (1997).
[9] F. Gulminelli and Ph. Chomaz, Phys. Rev. Lett.**82**, 1402 (1999).
[10] E. Bauge *et al.*, Phys. Rev. Lett. **70**, 3705 (1993).
[11] D. Durand, Nucl. Phys. **A630**, 52c (1998), and refs. therein.
[12] L. Beaulieu *et al.*, Phys. Rev. Lett. **77**, 462 (1996).
[13] N. Marie *et al.*, Phys. Lett. **B 391**, 15 (1997).
[14] J. Toke *et al.*, Phys. Rev. Lett. **75**, 2920 (1995).
[15] T. Lefort *et al.*, Phys. Rev. Lett. **83**, 4033 (1999).
[16] L. Beaulieu *et al.*, Phys. Lett. **B463**, 159 (1999)
[17] J.P. Bondorf, R. Donangelo, I.N. Mishustin and H. Schulz, Nucl. Phys. **A444**, 460 (1985).
[18] K. Kwiatkowski *et al.*, Nucl. Instr. Meth. A **360**, 571 (1995).
[19] W.-c. Hsi et al., Phys. Rev. C **60**, 034609-1 (1999).
[20] D.H. Boal, C.K. Gelbke and B.K. Jennings, Rev. Mod. Phys. **62**, 553 (1990).
[21] R. Trockel *et al.*, Phys. Rev. Lett. **59** 2844 (1987).
[22] R. Bougault *et al.*, Phys. Lett. **B232**, 291 (1989).
[23] Y.D. Kim *et al.*, Phys. Rev. Lett. **67**, 14 (1991); Y.D.Kim *et al.*, Phys. Rev. C **45** 338 and 387 (1992).
[24] M. Louvel *et al.*, Phys. Lett. **B320**, 221 (1994).
[25] D. Fox *et al.*, Phys. Rev. C **50**, 2424 (1994).
[26] T. Glasmacher *et al.*, Phys. Rev. C**50**, 952 (1994).
[27] R. Popescu *et al.*, Phys. Rev. C **58**, 270 (1998).
[28] G. Wang *et al.*, Phys. Rev. C **60**, 014603-1 (1999). **B460**, 31 (1999).
[29] T. Lefort *et al.*, Submitted to Phys. Lett. B and nucl-ex/9910017.

FIGURES

FIG. 1. Reduced velocity correlation functions generated for four different excitation energy per nucleon bins. IMF kinetic energy acceptance is in source frame is E_{IMF}/A = 1 - 10 MeV.

FIG. 2. Correlation functions for Z = 4-9 IMFs as a function of reduced velocity (open circles). IMF kinetic energy acceptance in the source frame is E_{IMF}/A = 2 - 10 MeV. Data gated on source E^*/A = 2.0 - 2.5 MeV (top), 4.5 -5.5 MeV (center)and 8.5 - 8.5 MeV (bottom). Solid and dashed lines are results of a Coulomb trajectory calculation for fit parameters indicated on figure.

FIG. 3. Dependence on E^*/A for source lifetime (bottom), thermally-driven expansion energy ϵ_r [29] (center) and probability of observing a given IMF multiplicity (top). In the bottom panel, the shaded area indicates the range of possible solutions (space-time) consistent with IMF observables. Solid line is an exponential fit to the ISiS results; dashed line a similar fit using heavy-ion data [11].

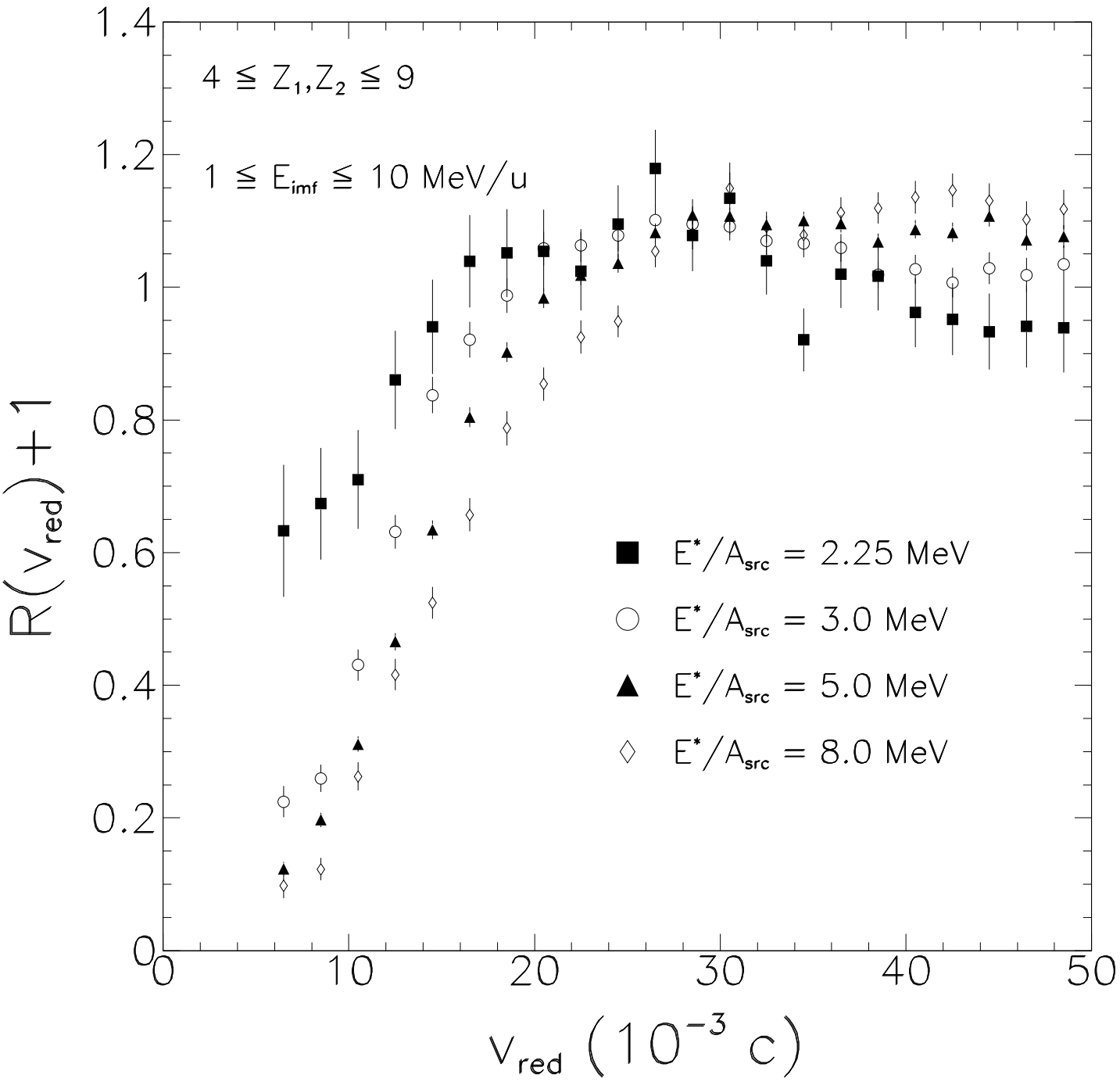

Fig. 1: L. Beaulieu *et al.*

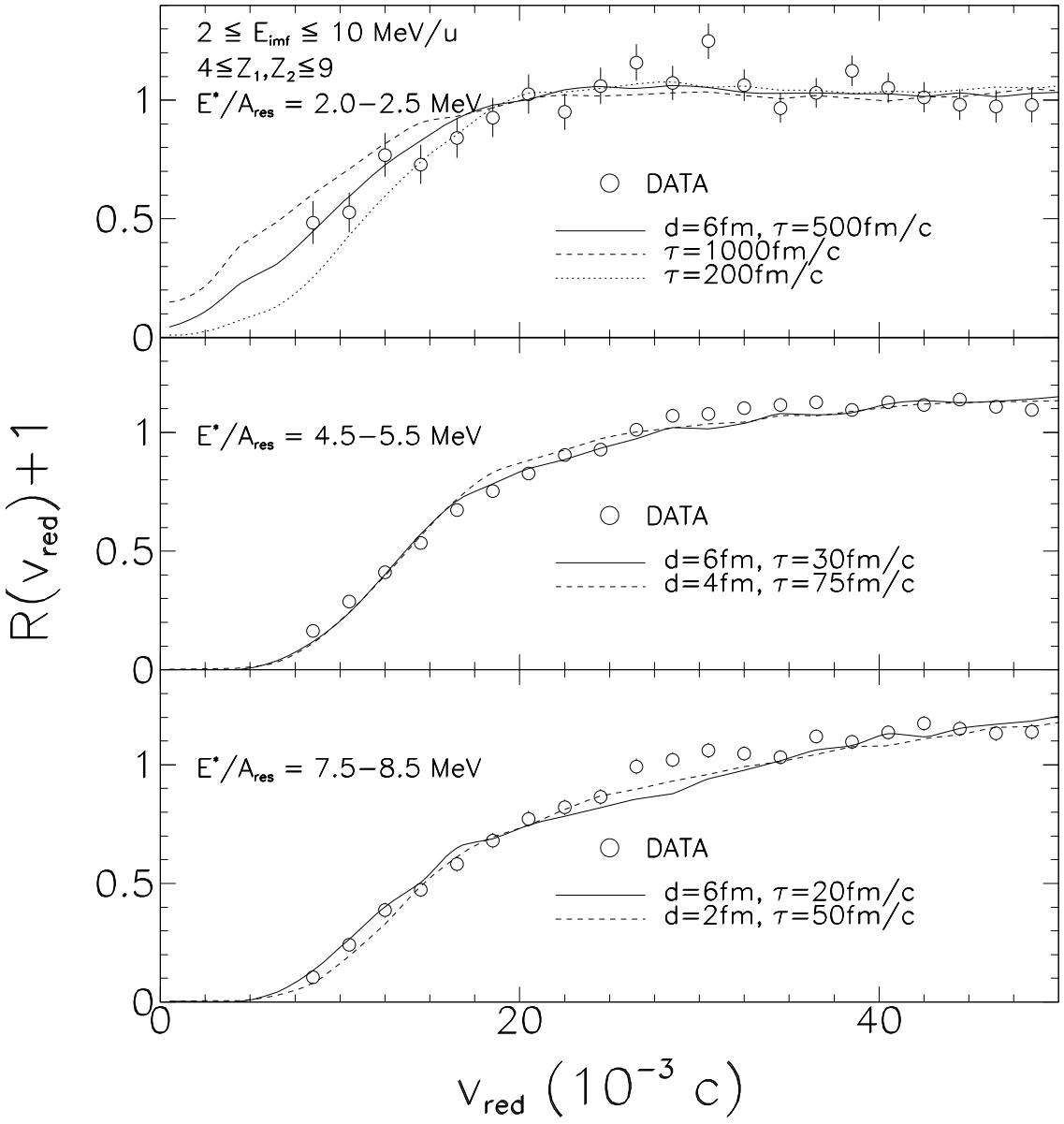

Fig. 2.: L. Beaulieu *et al.*

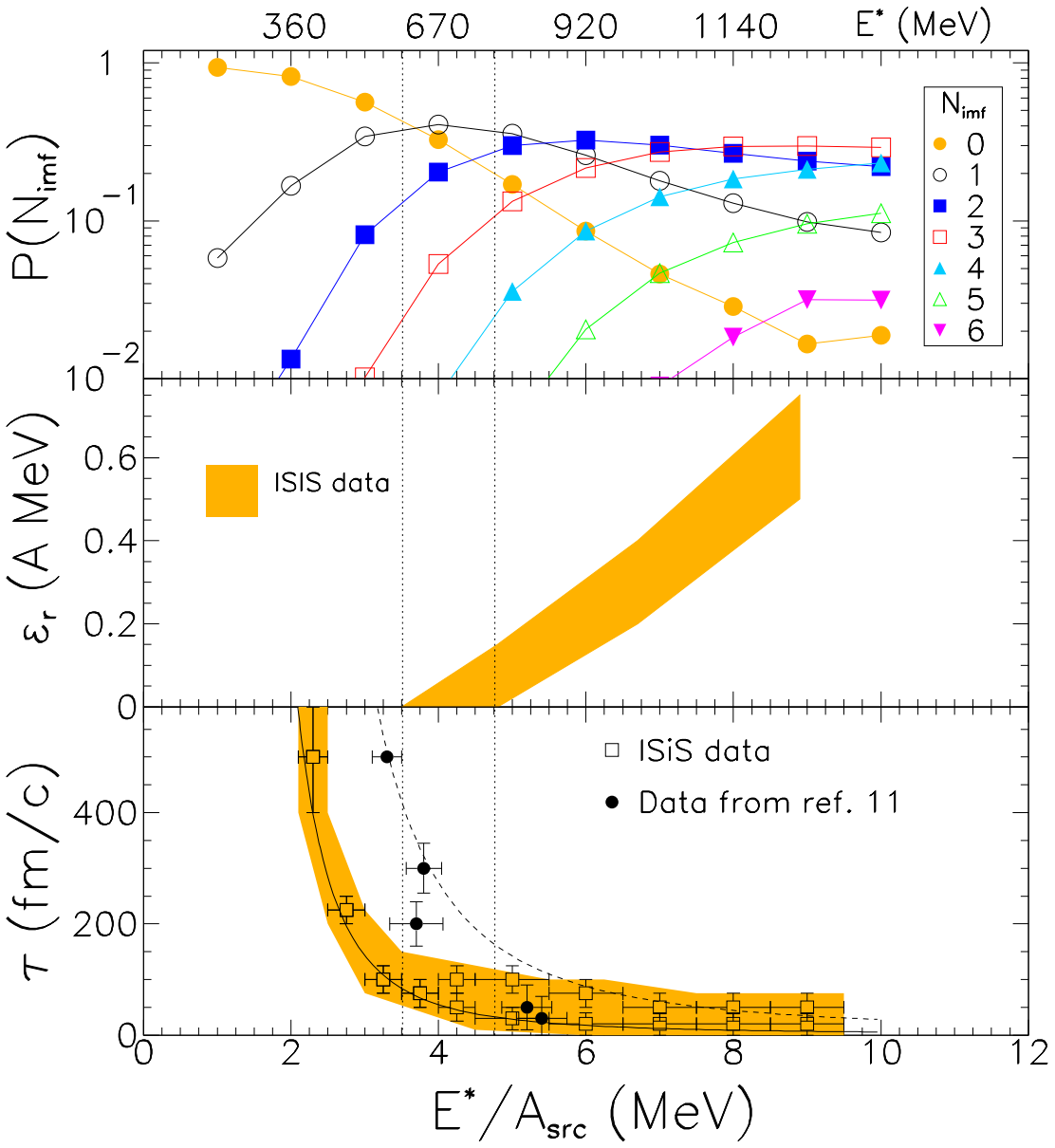

Fig. 3: L. Beaulieu *et al.*